Supplementary

S1. Study of FTIR Patterns of Organic Solvent (Without Metal Nitrates) Before Heating

The FTIR pattern of 2-MOE, acetic anhydride and a mixture of 2-MOE and acetic anhydride are shown in Figure S1.1. It is notable that the FTIR peaks of generic ester (at ~1730 cm^{-1}) and acetic acid (at ~1715 cm^{-1}) are absent in all three samples.

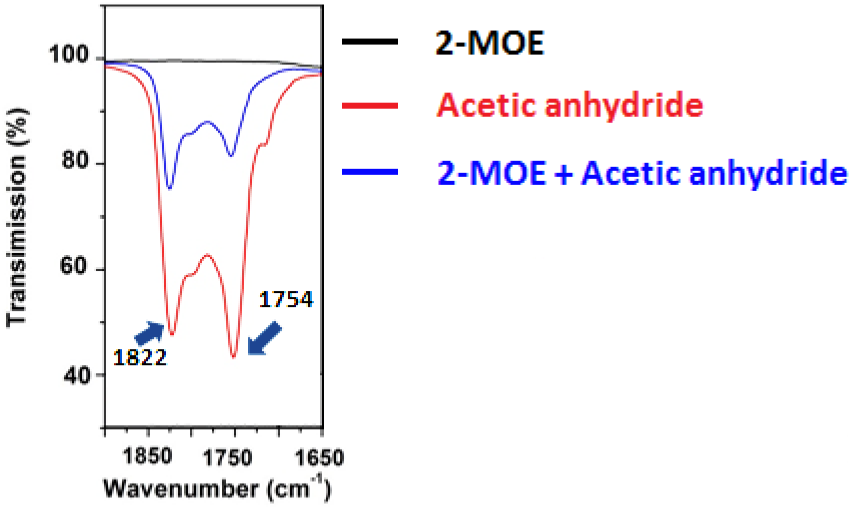

Fig. S1.1. FTIR spectra of 2-MOE, acetic anhydride and mixture of 2-MOE and acetic anhydride before heating

S2. Nuclear Magnetic Resonance Analysis

Precursor A1 and B1 without iron nitrate (because no NMR signal could be obtained if iron is present in the solution) was prepared for nuclear magnetic resonance (NMR, Avance III 400; Bruker, Germany) measurement to determine their initial organic molecular structures prior to any changes associated with subsequent heating and gelation. The compositions of precursor A1 and B1 are shown in Table S2.1. ^{1}H NMR spectra were obtained on neat mixtures with deuterated dimethyl sulfoxide (dmso-d6) in a capillary insert.

Table S2.1. Composition of starting materials of precursor solutions

	$Bi(NO_3)_3{\cdot}5H_2O$	2-MOE	Acetic anhydride
Precursor A1	0.015 mol	0.55 mol (43 ml)	-
Precursor B1	0.015 mol	0.29 mol (23 ml)	0.21 mol (20 ml)

The ^{1}H NMR pattern of bismuth nitrate solution in 2-MOE solvent without acetic anhydride (i.e. Precursor A1) is shown in Figure S2.1. The NMR peaks correlate well with the chemical composition of 2-MOE, namely CH_3-O-CH_2-CH_2-OH, that its functional groups of CH_3 (at ~3.2 ppm), CH_2 (at ~3.3 and ~3.5 ppm), and OH (at ~4.7 ppm) are clearly evident. No peaks of other functional groups containing H are present.

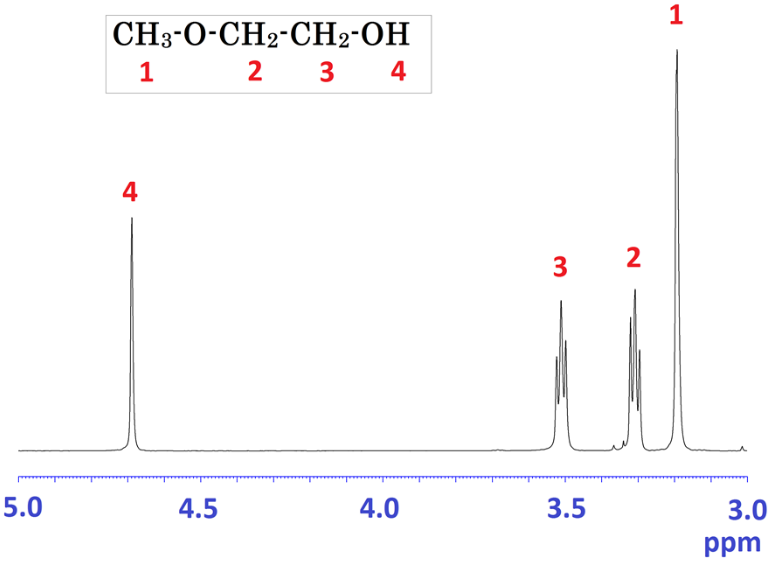

Fig. S2.1. NMR spectrum of as-prepared Precursor A1

The ^1H NMR pattern of the Precursor B1 is shown in Figure S2.2. In comparison with the NMR pattern of Precursor A1, the NMR pattern of the Precursor B1 contains more peaks, which is to be expected since it contains an additional organic species. According to the NMR spectra, besides the peaks corresponding to "**CH_3**-O-**CH_2**-**CH_2**-" of 2-MOE (peak 1, 2 and 3), additional peaks corresponding to a "**CH_3**-O-**CH_2**-**CH_2**-" structure in 2-methoxyethyl acetate (CH_3-CO-O-**CH_2**-**CH_2**-O-**CH_3**) (peak 5, 6 and 7) are also present. This latter structure, forms as a result of an esterification reaction between the 2-MOE and acetic anhydride (Eqn.3 given in Section 3.1.2). Peaks 9 and 8 around 1.8 ppm indicate H in "CH_3-" structures, which suggest the presence of acetic acid (**CH_3-**COOH) and 2-methoxyethyl acetate (**CH_3-**CO-O-CH_2-CH_2-O-CH_3) (as explained by Eqns. 2 and 3 in Section 3.1.2), respectively. Peak 4 at 5.8 ppm is attributed to "-OH" group which most likely on the 2-MOE.

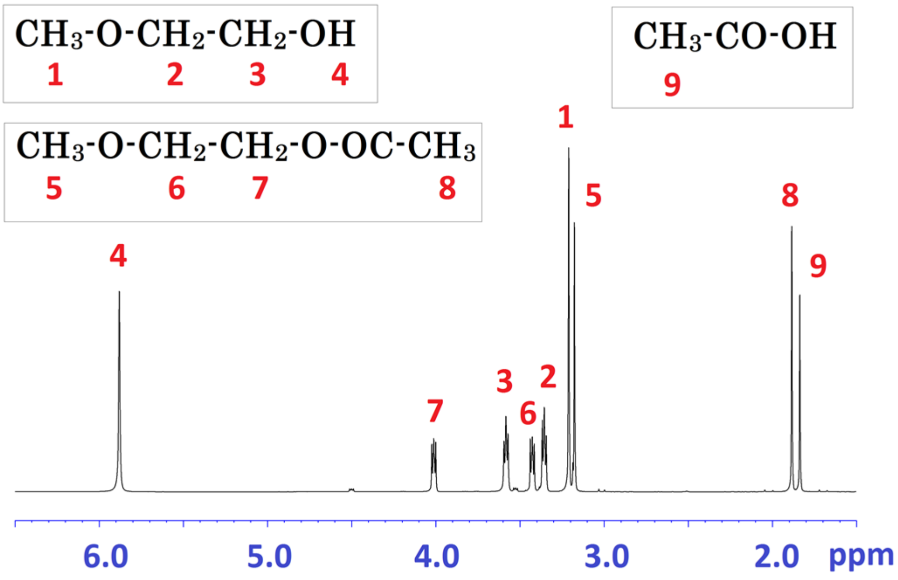

Fig. S2.2. NMR spectrum of Precursor B1

S3. Effect of Acetic Anhydride in Homogenous Gel Film Preparation

As mentioned in Section 3.1.2, the drying time of precursor A layer is shorter than that of precursor B layer under the sample heating condition. This is because Precursor B with acetic anhydride is with lower vapour pressure due to the formation of ester in the as-prepared precursor which can decrease the drying rate of solvent and reduce the opportunity of precipitate formation.

Using the same metal nitrates concentration (0.25 M stoichiometric), same deposition (spin coating at 3000 rpm for 30 seconds) and gelation condition (preheated at 70°C before spin coating) and same high-temperature crystallization conditions (at 650°C in oxygen for 30 mins), we prepared BFO thin film samples using precursor A and precursor B respectively. As shown in Figure S3.1 the surface of precursor A derived BFO thin film is comparatively rougher with a RMS roughness of approximately 4.1 nm, while the surface of precursor B derived BFO thin-film shows a smooth surface with a RMS of 1.9 nm. The larger roughness on Precursor A derived BFO thin films is due to the formation of inhomogeneous gel film (with precipitates) during spin coating and following gelation process (since the precursor A has a higher vapour pressure than precursor B).

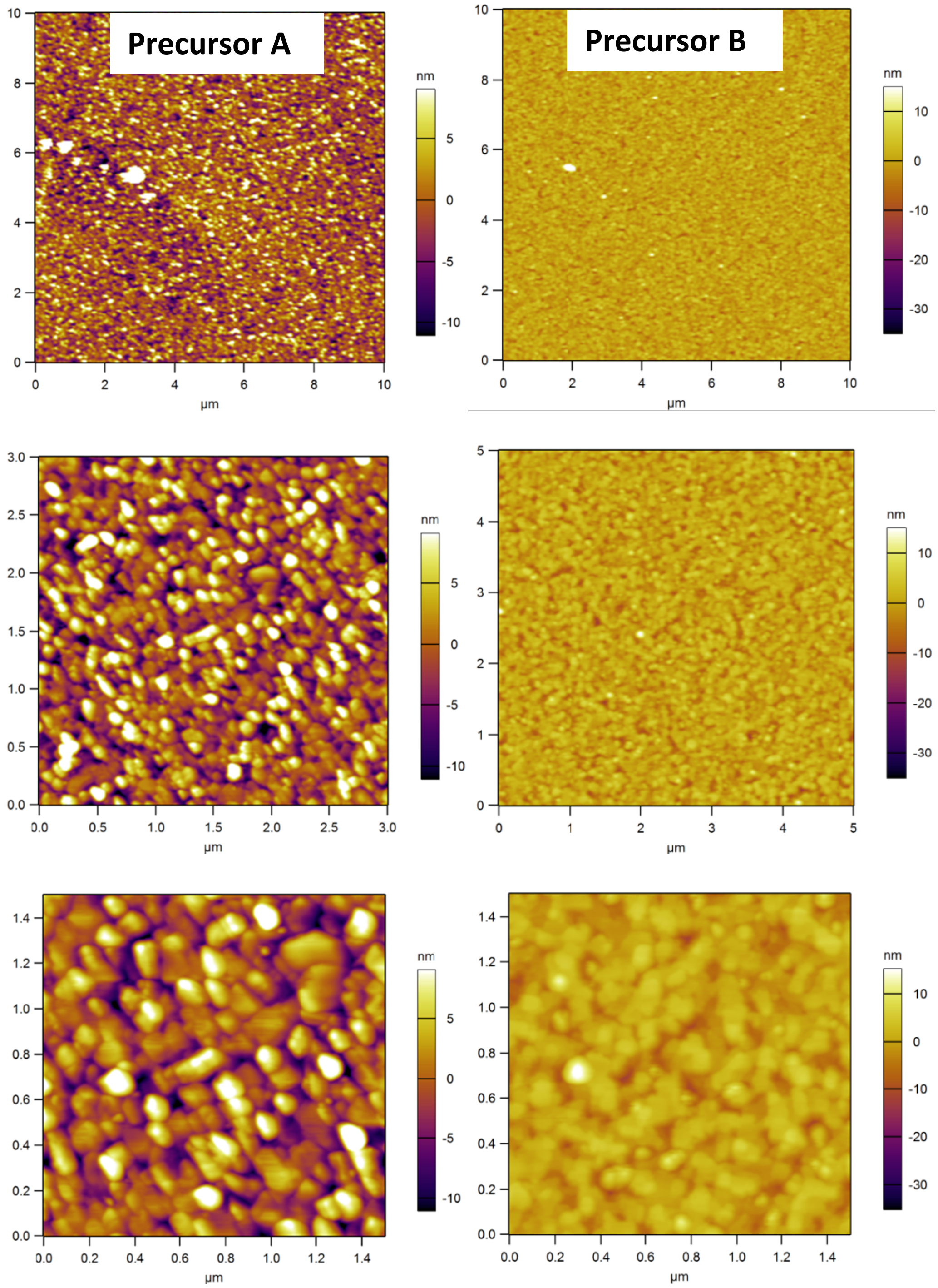

Fig. S3.1. AFM images of BFO thin films prepared by using Precursor A and Precursor B after crystallization at 650 °C for 30 minutes in an oxygen atmosphere

S4. Effect of Film Thickness

The effect of thickness on the gelation process was also studied. For this, thicker films were prepared by dropping 0.2 ml Precursor B on one edge of the glass substrate and then inclining the substrate at a shallow angle (<30º) to cover the surface with a uniform thick layer. The same sets of gelation heating conditions (i.e., temperature and time) as the thin-films were used for the thicker films.

Results of the study of the effect of gelation heating conditions on the topography of thicker film are summarized in Table S4.1. It is found that discrete precipitates formed at mild heating conditions (≤ 70ºC). Increasing the heating temperature to 80ºC and above resulted in extensive agglomeration of precipitates and a lack of gelation with the thick films having a powdery appearance (whereas clear gel thin films were obtained for ≥ 70ºC). Compared with the heating process for thin films, for thick films the drying time is expected to be much longer. Thus, the accumulation of heat energy in the precursor offers extra energy to the stabilized gel to overcome the potential repulsive barrier between each other thereby facilitating agglomeration[1]. In addition, cracking is found in thicker films after heating for a longer time (120 mins).

Table S4.1. Summary of effect of temperature conditions for gelation for thick films

(i) Effect of temperature

Heating temperature					
R.T	**50°C**	**60°C**	**70°C**	**80°C**	**90°C**
Precipitate (metal salts)	Precipitate (metal salts)	Precipitate (metal salts)	Precipitate (metal salts)	Agglomeration	Agglomeration

(ii) Effect of heating duration

Heating duration				
5 mins	**10 mins**	**20 mins**	**60 mins**	**120 mins**
Precipitate (metal salts)	Precipitate (metal salts)	Precipitate (metal salts)	Gel	Agglomeration & Cracking

[1] Brinker, C.J. and G.W. Scherer, *Sol-Gel Science: The Physics and Chemistry of Sol-Gel Processing*, Academic Press, Boston, 1990,

S5. Effect of Precursor Concentration

Starting precursors of three different metal nitrate concentrations (nominally 0.25 M, 0.35 M and 0.45 M) were prepared using stoichiometric Precursor B to study the effect of precursor concentration and the solvent vapour pressure on the microstructure of crystallized BFO thin-films. The compositions of the precursor solutions are summarized in Table 1 in the manuscript. The vapor pressures of the solvent in precursors of different metal nitrates concentrations can be calculated according to Raoult's Law in Eqn. S5.1:

$$P_{tot} = \sum_{i} P_i \chi_i \qquad \text{Eqn.S5.1}$$

Where:

P = Solvent's vapour pressure;

i = The ith component in the solvent;

χ = Mole fraction of the ith component in the solvent

As discussed in Section 3.1.2, in as-prepared precursor B, no acetic anhydride ($(CH_3\text{-}CO)_2O$) was found in the precursor after stirring and both acetic acid (CH_3COOH) and ester ($CH_3\text{-}O\text{-}CH_2\text{-}CH_2\text{-}O\text{-}OC\text{-}CH_3$) were detected suggesting reactions in Eqn.2 and Eqn.3 occur. The vapor pressures of 2-MOE ($CH_3\text{-}O\text{-}CH_2\text{-}CH_2\text{-}OH$), acetic acid ($CH_3COOH$), 2-methoxyethyl acetate ($CH_3\text{-}O\text{-}CH_2\text{-}CH_2\text{-}O\text{-}OC\text{-}CH_3$) and water at 20°C are 0.82 kPa, 1.53 kPa, 0.27 kPa, and 2.30 kPa, respectively. The vapour pressures of the precursor solutions (at 20°C) are given in Table S5.1 as a function of metal nitrate mass concentration, which were calculated assuming that Eqn.2 and Eqn. 3 occur equally (but, in any case, if Eqn.2 or Eqn. 3 occur first and to completion, then the vapour pressures of the resultant solutions will decrease or increase, respectively, by only ~2.5% relative to the values stated in Table S4 but, notably, the trend remains the same).

Table S5.1. Mass concentration and vapor pressure of precursor with various metal nitrate concentrations

	0.25 M	0.35 M	0.45 M
Mass Concentration (g/ml)	0.185	0.283	0.402
Vapour pressure (kPa, 20°C)	1.160	1.255	1.356

Thus, as the metal nitrate concentration increases, not only does the effective solids loading increase but also the total vapor pressure of the precursor solution (at 20°C). Owing to the former, the drying rate of the organic solvent would be expected to increase as the mass concentration increases. The accelerated loss of solvent would then shift the process in favour of precipitation over gelation. To further optimize the gel film quality, the experiment and discussion on the effect of preheating process on the thin film microstructure are given in S6 and Figure S6.1, where precursors with different concentrations are used.

S6. Prevention of Precipitation During Spin Coating

According to the discussion in Section 3.2.2 and Supplementary S5 for thin films, the precipitation of raw materials (metal salts) due to the onset of saturated mass concentration strongly depends on the solvent vapor pressure and the initial mass concentration of the cation. Thus, in addition to the control of film gelation heating temperature (as discussed in Section 3.2.2) and precursor concentration (as discussed in S5), the prevention of metal salt precipitates in the thin film before BFO high-temperature crystallization can also be achieved by increasing the precursor temperature to increase the precursor solubility and promote the initial gelation of precursor.

To prepare a thinner film, it is necessary to increase the spin velocity and spin time, which would increase the air flow rate on the precursor surface during spinning, thereby promoting the drying rate of solvent. To reduce metal nitrate precipitation during spinning, one effective method is to slightly increase the precursor temperature before/during spinning in order to increase the metal nitrate solubility in the precursor as well as promoting initial gelation. However, as we discussed above for Table S4.1, agglomeration precipitates start to form at 80 ºC in the thicker film due to the accumulation of heat in the precursor before drying. Thus any temperatures higher than 80 ºC may cause this sort of precipitation in the precursor. This is overcome by dropping the precursor on a preheated substrate (to 70 ºC) immediately before spin-coating. This pre-heating process effectively prevents the formation of precipitate agglomeration in the thinner films during spinning.

As shown in Figure S6.1, BFO thin films derived from precursors of different metal nitrate concentrations were prepared with and without preheating process. By comparing the topographies of BFO thin film, it is found that much smoother thin films are obtained when the substrates are preheated before deposition. The thin films without preheating process show a much higher root mean square roughness of 7.9-12.3 nm compared to the ones with preheating process (1.9-4.3 nm) due to the precipitates formed during spinning. The shapes of these precipitates change with the precursor concentration such that a small size granular precipitates are found on the 0.25 M precursor derived BFO thin films. This kind of precipitates is similar to the one as shown in Figure 7 (0.25 M, 60°C). The rougher surfaces of 0.35 M and 0.45 M precursor derived BFO thin films should be due to the formation of complex precipitates comparable to the Figure 7 (0.35 M, 0.45 M, 60°C).

In addition, by comparing the topographies of BFO thin films prepared by precursors with different metal nitrate concentrations, it is found that the roughness increases with the increase of precursor metal nitrate concentration. In the group with preheating process, the root mean square (RSM) roughness increases from 1.9 nm (0.25 M) to 4.0 nm (0.35 M) to 4.3 (0.45 M). The same tendency is observed for the group without any preheating, but with a relatively higher roughness for all 0.25 M, 0.35 M and 0.45 M thin films. This result is consistent with the discussion in Section 3.2.2 and S5, that the drying rate of 0.45 M is higher than that of the 0.25 M precursor due to its higher vapour pressure.

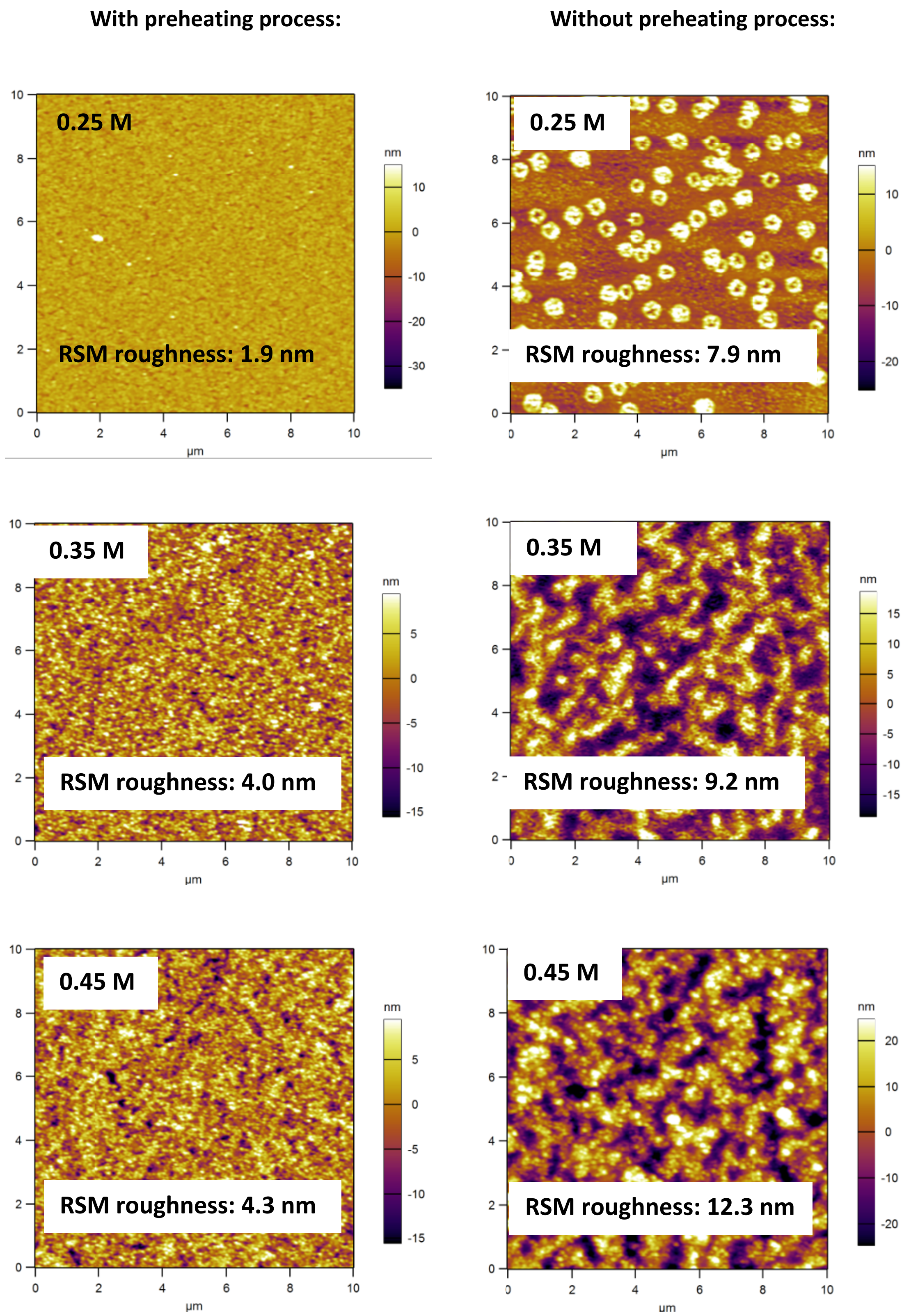

Figure S6.1. AFM topographic images of BFO/STO(001) thin films prepared by stoichiometric Precursor B with various metal salts concentrations (0.25 M, 0.35 M, 0.45 M) with or without preheating process after crystallized at 650°C in an oxygen atmosphere

S7. Energy-Dispersive X-ray Spectroscopy (EDS) Analysis on the BFO Thin Films

Figure S7.1 show the EDS analysis in the cross-section of the 150 nm BFO/LSMO/STO(001) thin film. The Fe: Bi ratio in 150 nm is 55.5:44.5 in average (data of 14 points from the cross-section were acquired). The deficiency of Bi in the thicker film is due to the longer annealing duration for the multi-layer deposition process.

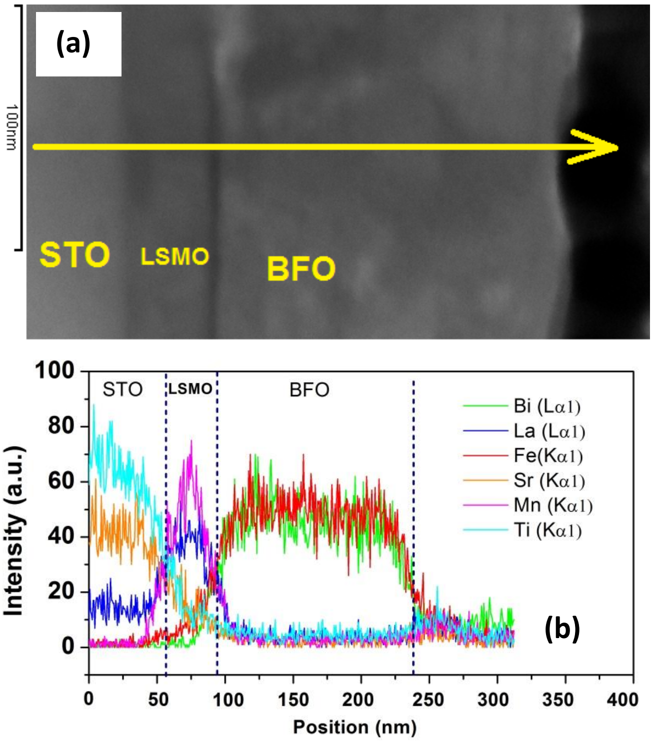

Point	Fe (at.%)	Bi (at.%)
1	54.85	45.15
2	55.63	44.37
3	55.18	44.82
4	55.89	44.11
5	54.56	45.44
6	56.8	43.2
7	54.61	45.39
8	56.71	43.29
9	55.44	44.56
10	56.71	43.29
11	56.57	43.43
12	56.29	43.72
13	53.52	46.48
14	53.52	46.48
Mean	55.45	44.55
Standard Error	0.29	0.29

Figure S7.1. ESD analysis on the element distribution in the film thickness (a) Cross-section image of BFO/LSMO/STO thin film by TEM; (b) EDS analysis on the cross-section of BFO/LSMO/STO thin film. Table shows the Fe:Bi ratio on the cross-section of BFO thin films by point EDS.

Figure S7.2 shows the AFM images of BFO thin films derived from gel film with precipitates (See Figure S6.1 and Figure 9(b)), along with the results of EDS point analysis in the specific regions. The areas derived from gel matrix shows a smooth and homogenous morphology with Bi-deficiency (Fe:Bi=52.6:47.4). The precipitates are either clear Bi-rich (Fe:Bi=41.5:58.5) phases or Fe-rich (Fe:Bi=58.0:42.0) phases. The errors given in this measurement in below figure are standard errors.

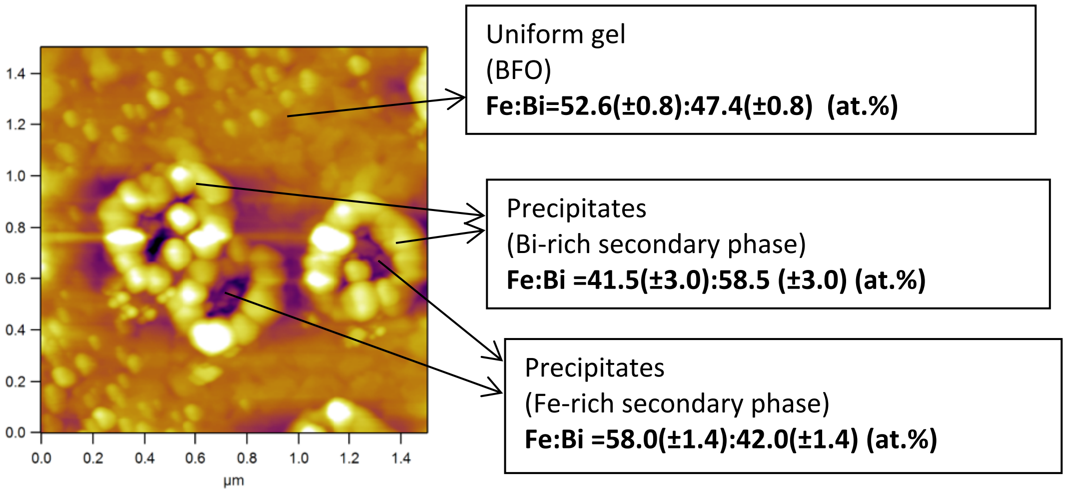

Uniform gel
(BFO)
Fe:Bi=52.6(±0.8):47.4(±0.8) (at.%)

Precipitates
(Bi-rich secondary phase)
Fe:Bi =41.5(±3.0):58.5 (±3.0) (at.%)

Precipitates
(Fe-rich secondary phase)
Fe:Bi =58.0(±1.4):42.0(±1.4) (at.%)

Figure S7.2. AFM images and composition analysis of BFO thin films derived from gel film with precipitates

S8. Gelation process

Gelation process at 90°C as a function of time are shown in Figure S8.1. Films were prepared by dropping Precursor B on glass substrates and the substrates then inclined to 90°C to cover the surface with a uniform layer of solution. This preparation process is same as the one used to study gelation mechanism (See Figures 7-8 in Section 3.2.1 in manuscript). Compared with heating at 70°C (See Figure 8 in manuscript), homogenous gel films with no precipitates are observed for all the films heating at 90°C (1 min to 20 mins). That is, this time of 1 minute is sufficient for the 90°C process due to accelerated effect on gelation. Therefore from a practical perspective, 90°C process is a lot more attractive for practical thin-film preparation.

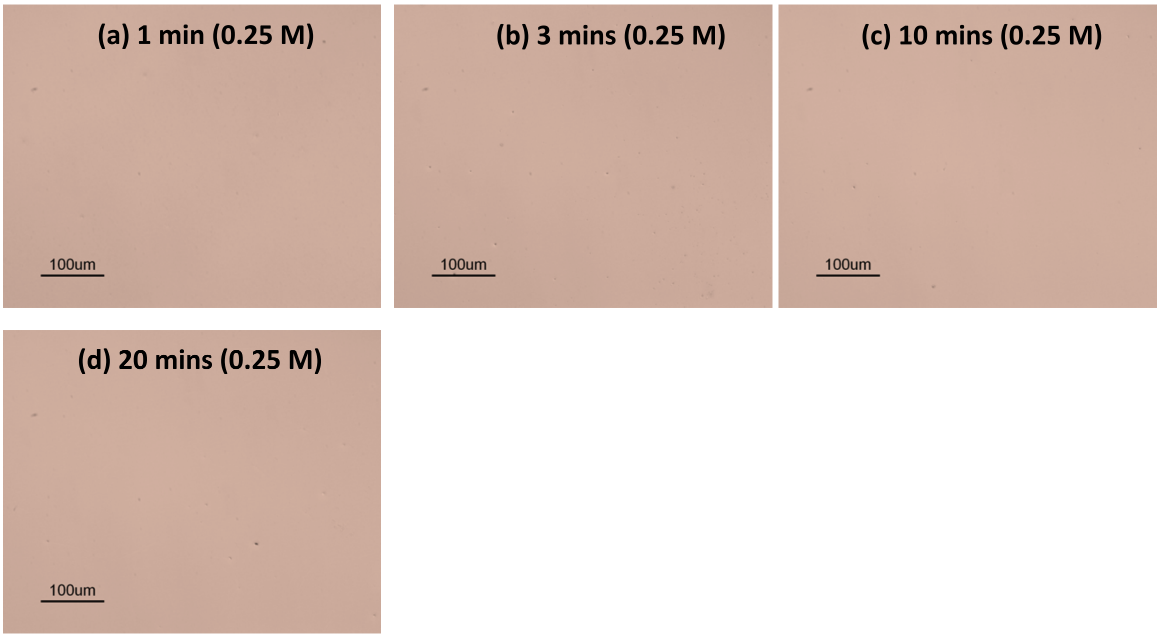

Fig. S8.1. Microscopic structures of as-deposited thin films (prepared by 0.25 M Precursor B) after heating at 90°C for various durations ((a) 1 minute; (b) 3 minutes; (c) 10 minutes; (d) 20 minutes), followed by drying at room temperature in an ambient air for 12 hours. Films are prepared by dropping Precursor B on glass substrates and the substrates then inclined to 90° to cover the surface with a uniform layer of solution.

BFO thin-films device for ferroelectric properties measurement were prepared by spin coating process, which leads to a more uniform and thinner films compared with films for gelation investigation (as shown in Figure 8 and Figure S8.1). To further confirm that 90 °C is a suitable gelation conditions for the thinner films prepared by spin coating, films were prepared by dropping the Precursor B on the 70°C preheated glass substrates, followed by spin coating at 3000 rpm for 30 s, and heating at 90°C for gelation. Optical images of the gel-films processed at 90°C as a function of time (1 min and 10 mins) are shown in Figure S8.2. Homogenous gel films with no precipitates are observed for both films, indicating that 1 min is sufficient for the gelation of spin-coated thin-film. Thus, this heating condition was used in this report to prepare BFO thin film devices for ferroelectric property characterizations.

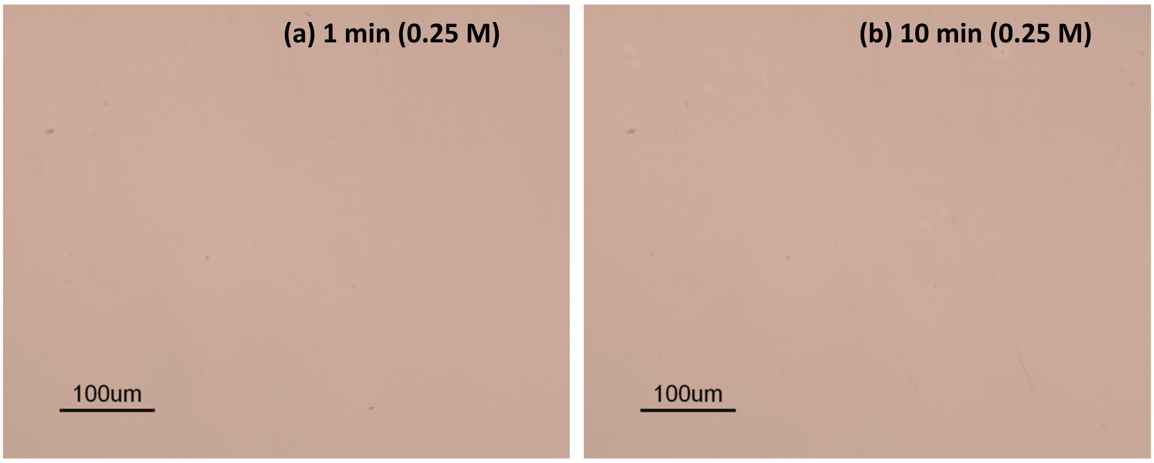

Fig. S8.2. Microscopic structures of as-deposited thin films (prepared by 0.25 M Precursor B) after heating at 90°C for (a) 1 minute and (b) 10 minutes, followed by drying at room temperature in an ambient air for 12 hours. The films were prepared by dropping the Precursor B on the 70°C preheated glass substrates, followed by spin coating at 3000 rpm for 30 s, and heating at 90 degree for gelation.